LETTERS

Transmission resonances through aperiodic arrays of subwavelength apertures

Tatsunosuke Matsui[1]*, Amit Agrawal[2]*, Ajay Nahata[2] & Z. Valy Vardeny[1]

Resonantly enhanced light transmission through periodic subwavelength aperture arrays perforated in metallic films[1] has generated significant interest because of potential applications in near-field microscopy, photolithography, displays, and thermal emission[2]. The enhanced transmission was originally explained by a mechanism where surface plasmon polaritons (collective electronic excitations in the metal surface) mediate light transmission through the grating[1,3]. In this picture, structural periodicity is perceived to be crucial in forming the transmission resonances. Here we demonstrate experimentally that, in contrast to the conventional view, sharp transmission resonances can be obtained from aperiodic aperture arrays. Terahertz transmission resonances are observed from several arrays in metallic films that exhibit unusual local *n*-fold rotational symmetries, where $n =$ 10, 12, 18, 40 and 120. This is accomplished by using quasicrystals with long-range order, as well as a new type of 'quasicrystal approximates' in which the long-range order is somewhat relaxed. We find that strong transmission resonances also form in these aperiodic structures, at frequencies that closely match the discrete Fourier transform vectors in the aperture array structure factor. The shape of these resonances arises from Fano interference[4] of the discrete resonances and the non-resonant transmission band continuum related to the individual holes[5]. Our approach expands potential design parameters for aperture arrays that are aperiodic but contain discrete Fourier transform vectors, and opens new avenues for optoelectronic devices.

Periodicity, or the lack of it, is of fundamental importance in a broad range of science and engineering disciplines. In particular, two-dimensional (2D) aperture arrays can be described in terms of long-range order, short-range order, and local rotational symmetry that may be revealed in the Fourier transform structure factor. Several 2D array classes exist, including: (1) periodic lattices having both long-range and short-range order, and discrete Fourier transform vectors, but their *n*-fold rotational symmetry in real and reciprocal space is limited to $n = 2, 3, 4$ and 6; (2) quasicrystals with long-range order but no short-range order, but their discrete Fourier transform vectors possess unusual *n*-fold rotational symmetry with $n = 5$, 8, 12, and so on[6]; (3) aperiodic structures having no long-range or short-range order, but their structure factor may contain a number of discrete Fourier transform vectors with even more unusual *n*-fold rotational symmetry; and finally (4) randomly distributed holes with no discrete Fourier transform vectors at all. Patterns that fall into categories (2) and (3) can be referred to generically as aperiodic structures, although quasicrystals[6] are unique in that their patterns can be developed using well-defined algorithms. The lack of periodicity in these two categories excludes the possibility of describing them using well-established analytical tools (such as Brillouin zones and the Bloch theorem) that are unique to Bravais lattices.

In this investigation, we examine resonantly enhanced transmission of the terahertz (THz) electric field through metallic films perforated with several 2D aperiodic aperture arrays using THz time-domain spectroscopy (see Supplementary Information)[7]. Two-dimensional aperture arrays were fabricated in an $\sim$5 cm$\times$5 cm area of 75-μm-thick free-standing stainless steel metal foils. Six different aperture array sample sets were fabricated with differing hole diameter, nearest-neighbour hole distance, and local rotational symmetry. Most of these structures were designed to have the same fractional aperture area of $\sim$12%. One set of samples consisted of randomly distributed holes; the other five sets contained some samples that were in the form of 2D quasicrystals exhibiting five-fold[8] and 12-fold[9] rotational symmetry, and some samples that were novel quasicrystal approximates exhibiting 18-, 40- and 120-fold rotational symmetry. 2D fast Fourier transform (FFT) was applied to the individual array patterns to determine their underlying geometrical structure factor.

Figure 1 summarizes our studies on perforated metallic films with randomly distributed apertures for which the FFT contains no discrete components. Figure 1a shows the THz transmission spectra, $T(v)$, up to $v = 0.5$ THz for three perforated films with a differing number of apertures. In each case, the hole diameter, D, is 0.4 mm. $T(v)$ increases at high frequencies, reaching a broad maximum that scales linearly with the number of holes in the film (Fig. 1a inset), indicating that it is due to transmission through uncorrelated individual holes. Figure 1b shows $T(v)$ for three different perforated films in which D varies, and the number of holes was altered to keep the fractional aperture area constant at $\sim$12%. It is apparent that $T(v)$ increases at an onset frequency that scales with D (Fig. 1b inset). Therefore, the increase in $T(v)$ at short wavelengths can be attributed to a waveguide cut-off phenomenon at frequency v_c, where the propagation of electromagnetic radiation through the holes is increasingly suppressed for $v < v_c$. Also, the maximum transmission, T_{max}, of $\sim$20% is greater than that predicted from the fractional aperture area ($\sim$12%).

The origin of these deviations from theory[10] was recently explained using an analytical approach based on induced magnetic and electric dipoles on either side of the metallic film through an individual hole[5]. The good fit between our experimental $T(v)$ spectrum seen in Fig. 1a and this model (using $D = 0.42$ mm) validates both the assumption that the transmission spectrum is due to uncorrelated holes, and the model calculation. Thus, when electromagnetic radiation is incident on a perforated metallic film, it scatters from the holes into free space, as well as into surface waves on the metal–air interfaces[11]. If more than one aperture is fabricated in the metal film, it is conceivable that the scattered surface waves would interfere. For films containing randomly distributed holes, we would not expect strong interference, explaining the lack of sharp resonances in $T(v)$. The situation is very

[1]Physics Department, [2]Department of Electrical and Computer Engineering, University of Utah, Salt Lake City, Utah 84112, USA.
*These authors contributed equally to this work.

different, however, for films that show discrete Fourier transform vectors in their structure factor even with aperiodic structure, such as quasicrystals and their approximates.

Figure 2 summarizes our studies on 2D quasicrystal aperture arrays fabricated in metal films that exhibit local five-fold and 12-fold rotational symmetry. Figure 2a shows a Penrose-type quasicrystal[12] in which the apertures were fabricated at the vertices of the thin and thick rhomb tiles having tile side length d_3 (Fig. 2a). Figure 2b shows the geometrical structure factor of the Penrose quasicrystal, which possesses ten-fold rotational symmetry about the centre, with four series of circular spots about it. These spots can be associated with vectors **F** in reciprocal space, referred to as reciprocal vectors[8], that satisfy the relation $\exp(i\mathbf{F}\bullet\mathbf{R}) = 1$ for all the apertures having coordinates **R**. In contrast to the case of a periodic pattern such as a lattice, in which the structure factor is in the form of a Bravais lattice spanned in 2D by two primitive vectors[1], the quasicrystal reciprocal vectors may be conveniently indexed according to their distance from the centre. These distances, in turn, may be related directly to specific real-space distances in the Penrose structure[8,12] (Fig. 2a and Supplementary Information).

Figure 2c shows $T(\nu)$ of three perforated films with different values of d_3, keeping the fractional aperture area at 12%. Each $T(\nu)$ consists of three well pronounced transmission bands (or resonances) referenced as $\mathrm{F}^{(1)}$, $\mathrm{F}^{(2)}$ and $\mathrm{F}^{(3)}$ that are directly related to the reciprocal vectors in Fig. 2b, as well as a less pronounced resonance $\mathrm{F}^{(4)}$. We note that the resonance frequencies, $\nu^{(i)}$, scale with the magnitude of the corresponding reciprocal vectors in Fig. 2b, clearly demonstrating that the reciprocal vectors are in fact the wave-vectors **k** at resonance (Supplementary Information).

To demonstrate that transmission resonances are more generally observed from quasiperiodic aperture arrays, Fig. 2d shows a structure that exhibits local 12-fold rotation symmetry[13]. Figure 2e shows that the FFT of this structure contains five series of reciprocal vectors,

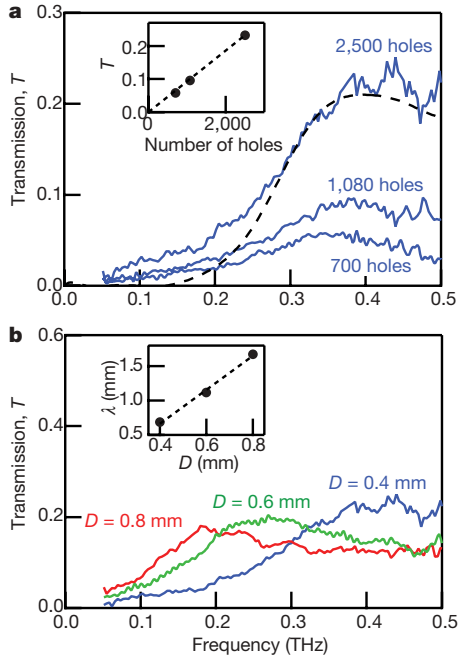

Figure 1 | THz electric field transmission, $T(\nu)$, through random apertures in stainless steel foils. a, Data for three films with different numbers of holes having diameter $D = 0.4$ mm; the dashed line through the data points is a fit using the individual hole transmission model of ref. 5 with $D = 0.42$ mm. The inset shows the transmission maximum at 0.4 THz versus the number of holes in the film. **b**, Perforated films with apertures of different D with the number of holes adjusted to keep the fractional aperture area constant at ~ 12%; the inset shows the dependence of the onset wavelength versus D.

referred to as $\mathbf{T}^{(i)}$, about the centre point. The magnitudes of these reciprocal vectors correspond to real distances in the quasicrystal structure (Fig. 2e and Supplementary Information).

Figure 2f shows typical $T(\nu)$ spectra of this quasicrystal structure having two different aperture diameters in the metal film. We see three primary resonances that correspond to the reciprocal vectors $\mathbf{T}^{(1)}$, $\mathbf{T}^{(3)}$ and $\mathbf{T}^{(4)}$, as summarized in Supplementary Table 2. $T(\nu)$ also contains several accompanying anti-resonances, each on the high-energy side of each resonance band. Importantly we note that the lowest resonance, $\mathrm{T}^{(1)}$, is hardly seen in Fig. 2f(bottom trace) for $D = 0.35$ mm; in turn, the $\mathrm{T}^{(3)}$ and $\mathrm{T}^{(4)}$ resonances cannot be clearly identified in Fig. 2f (top trace) for $D = 0.58$ mm. In addition, the resonance $\mathrm{T}^{(1)}$ shifts to higher frequency when D decreases, whereas the anti-resonance frequency remains unchanged. Recently Sun *et al.* reported enhanced transmission through aperture arrays based on eight-fold quasicrystals at optical frequencies[14]. However, they concluded that both long-range order and periodicity are very important for substantial surface plasmon polariton (SPP) coupling, and also did not observe the important anti-resonance features in $T(\nu)$. In contrast, it is clear from our findings that periodicity is not crucial for observing transmission resonances in perforated films. Additionally, we have found that the anti-resonances are crucial in determining the resonance shape in $T(\nu)$. Also, another recent report[15] found enhanced transmission bands for a Penrose quasicrystal in the visible spectral range, but claimed that the resonances are broader than those based on periodic structures. Our data show, however, that at least in the THz range, the transmission resonances of quasicrystal structures are as sharp as those based on periodic arrays.

Numerous models have been put forward to explain the phenomenon of resonantly enhanced transmission through periodically perforated metallic films, but a general consensus has not emerged yet. The transmission resonances with aperiodic arrays found here may have the potential to clarify the underlying physics of the anomalous transmission phenomenon. In the model most commonly used to describe this effect[1,3], the incident light couples to SPP excitations with resonant wave-vector $\mathbf{k}_{\mathrm{SPP}}$ associated with the aperture array grating, via the quasi-momentum conservation rule:

$$\mathbf{k}_{||} + \mathbf{k}_{\mathrm{SPP}} = \mathbf{G}^{(i)} \qquad (1)$$

Here, $\mathbf{k}_{||} = 2\pi\sin\theta/\lambda$ is the light wave-vector parallel to the film surface, θ is the angle between the light wave-vector and the surface normal, and $\mathbf{G}^{(i)}$ is a reciprocal lattice vector. Whereas equation (1) is typically associated with arrays that are strictly periodic, such arrays in practice are always finite, and thus $\mathbf{G}^{(i)}$ are not very well defined. For sufficiently large arrays, however, this equation appears to adequately describe the underlying physics. Quasicrystals are aperiodic but exhibit long-range order. Nevertheless, as with finite periodic arrays, an appropriately modified version of equation (1) may still describe the transmission resonance properties, except that the $\mathbf{G}^{(i)}$ would be replaced by the discrete Fourier transform vectors in the structure factor, namely the reciprocal vectors. Thus sharp transmission resonances would be formed for any structure that contains reciprocal vectors in its FFT geometry.

Transmission resonances associated with aperture arrays on metal films studied with visible light are characterized by broad lineshapes that are largely symmetric about the spectral peaks. Although anti-resonance features are discernible, they are not sharply defined[16]. In contrast, the resonances observed here in the THz range are sharply asymmetric and characterized by well-defined anti-resonances on the high-frequency side. We propose that these spectral features arise from the interference between discrete resonances caused by the diffraction from the aperture array, and the broad (continuum) transmission spectrum associated with the individual apertures on the metal film (Fig. 1). This interaction is well described by Fano interference[17]. It can be readily recognized that the resonances in $T(\nu)$ (Fig. 2c and f) are superimposed on the continuum spectrum of the

individual apertures (Fig. 1a). Fano interference also explains the relative enhancements observed in Fig. 2f. For small D, the continuum band blue-shifts to higher frequencies (Fig. 1b), and thus discrete resonances having higher frequencies become more apparent. The reverse situation occurs at large D, in which case the continuum band red-shifts (Fig. 1b), and thus discrete resonances with lower frequencies are better resolved.

Fano interferences are known to result in anti-resonances on the high-frequency side of the resonance bands[4,18]. Although more theoretical work is needed to elucidate the coupling between the discrete resonances and the continuum band, it is clear that because of the Fano interference, the apparent peak frequencies are red-shifted with respect to the true resonances[4,19], and thus may change with D. In contrast, the anti-resonance frequencies remain unchanged[17].

We demonstrate here that sharp transmission resonances are also formed in metal films perforated with a much broader range of aperiodic arrays, such as 'approximate' 2D quasicrystal structures, for which geometric tilings are not available or known. Figure 3a shows the design procedure[20] for an 'approximate' 18-fold 2D quasicrystal patterned on the metal film. We note that the distances, d_i,

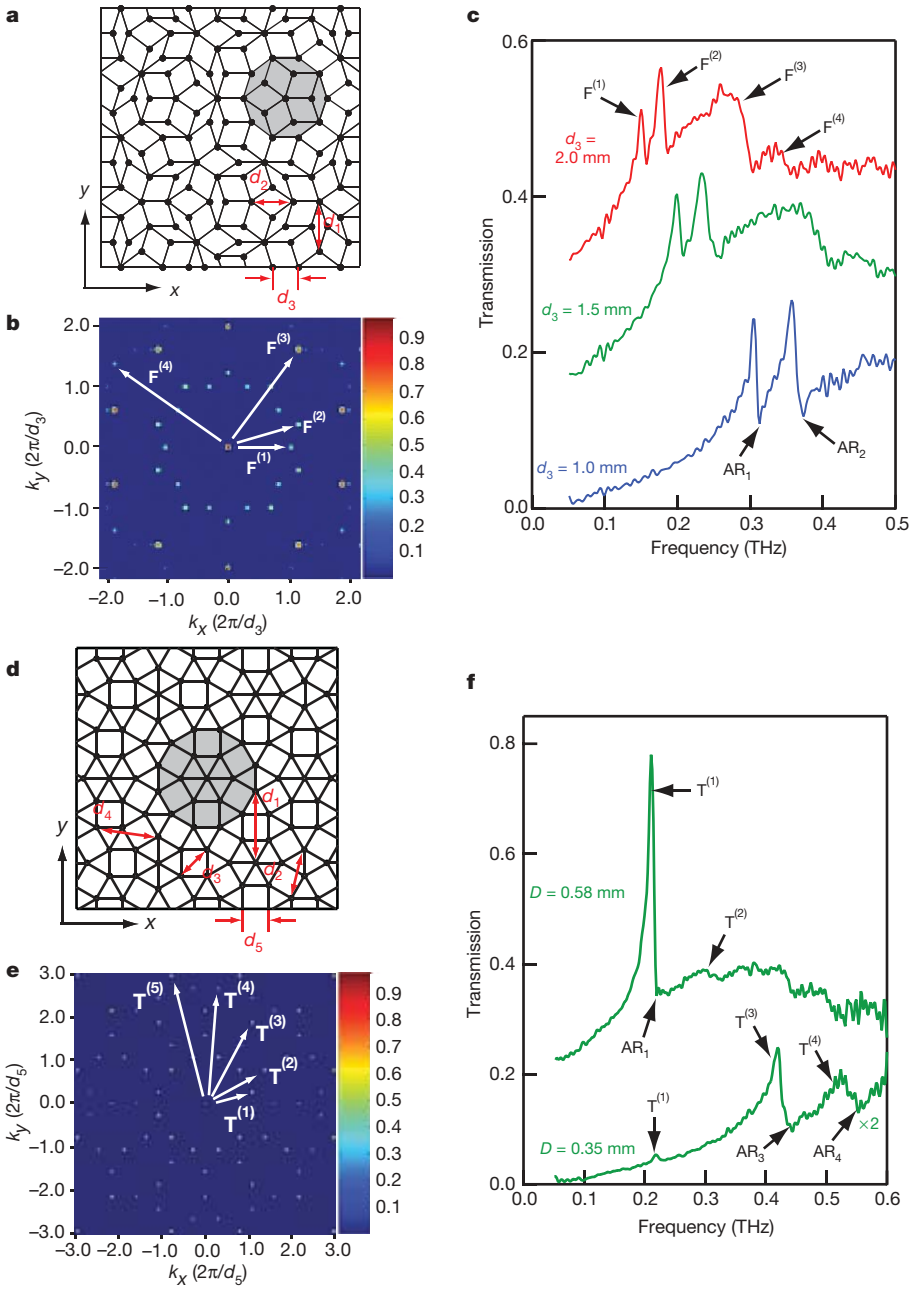

Figure 2 | THz time-domain spectroscopy studies of stainless steel foils perforated with apertures patterned in 2D quasicrystal structures. **a**, A Penrose quasicrystal exhibiting local five-fold rotational symmetry (shaded area) with apertures at the vertices, constructed of thin and thick rhomb tiles. The distances, d_i, between the vertices are assigned, with d_3 referring to the length of the rhomb side. **b**, The structure factor of the quasicrystal in **a** calculated using a 2D FFT. The reciprocal vectors, $\mathbf{F}^{(i)}$, which exhibit ten-fold rotational symmetry, are assigned. **c**, $T(\nu)$ of three Penrose type quasicrystal perforated films with different rhomb side lengths, d_3, showing resonances $F^{(i)}$ and anti-resonances AR_i. **d**, Same as in **a** but for a 2D quasicrystal structure with local 12-fold rotational symmetry and dominant tile length d_5. **e**, The structure factor of the quasicrystal in **d**; the reciprocal vectors, $\mathbf{T}^{(i)}$, with 12-fold rotational symmetry are assigned. **f**, $T(\nu)$ of two quasicrystals with 12-fold rotational symmetry perforated in metal films with a hole diameter $D = 0.35$ mm (×2) and 0.58 mm, respectively. For both spectra, the side length was $d_5 = 1.5$ mm, and the resonances $T^{(i)}$ and anti-resonances AR_i are denoted.

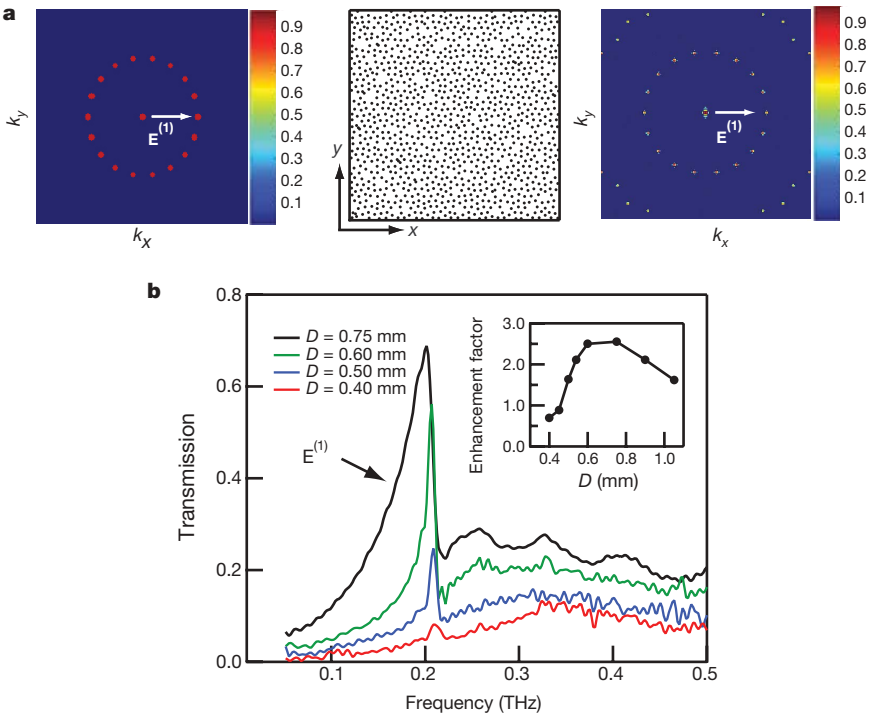

Figure 3 | Design and THz time-domain spectroscopy studies of stainless steel foils perforated with 2D aperiodic aperture arrays. a, Numerical approach for obtaining aperiodic arrays. Left panel, the desired 2D diffraction pattern for 18-fold rotational symmetry. Centre panel, the discretized magnitude of the inverse Fourier transform. The inverse Fourier transform is continuous and therefore requires threshold cutting to obtain discrete points. These points are the locations of the apertures in real space. Right panel, Fourier transform of the real space aperture locations for obtaining the final structure factor properties. **b**, Electric field transmission spectra of four aperiodic arrays with 18-fold rotational symmetry perforated in metal films with aperture diameters of $D = 0.4$, 0.5, 0.6 and 0.75 mm, respectively; the resonant band $E^{(1)}$ is assigned. In each case, the average hole spacing was 1.5 mm. The inset shows the enhancement factor (that is, the ratio of $E^{(1)}$ peak magnitude to the saturated transmission magnitude at high v) as a function of D.

between apertures in more traditional quasicrystals created using tiling are well-defined, in contrast to the aperiodic structures obtained using the numerical procedure described here. Therefore, the approximate quasicrystal structures are not quasiperiodic, but more correctly aperiodic. Nevertheless, well-defined resonances in $T(v)$ still exist.

Figure 3b shows $T(v)$ of four 18-fold aperiodic structures with various aperture diameters, in which the average hole spacing is 1.5 mm. In each case, we see only one prominent transmission resonance, $E^{(1)}$ at 0.21 THz, which is in agreement with the numerically obtained reciprocal vectors in the structure factor shown in Fig. 3a (panel #3). Furthermore, there is an apparent monotonic increase in the magnitude of the transmission peak with increasing D up to 750 μm. The inset of Fig. 3b summarizes the dependence on D of the ratio of the resonance peak magnitude to the continuum band saturation level (that is, the enhancement factor). We find that the optimal diameter for transmission enhancement is ~750 μm. This may be explained as follows: as D increases, the individual aperture continuum band in $T(v)$ red-shifts (Fig. 1b), thereby increasing the prominence of low-frequency transmission resonances. This demonstrates the intimate relation that exists in $T(v)$ between the discrete resonances and the continuum band. At $D > 750$ μm, where the apertures no longer can act as cut-off waveguides, the enhancement factor decreases. Finally, as with quasicrystal structures, we again see that the resonant frequency $E^{(1)}$ shifts with the aperture diameter, D, while the corresponding anti-resonance frequency does not.

The true value of the numerical approach described here is that it allows for the generation of arbitrary aperiodic arrays with exotic structures that form a variety of designed transmission properties. Using this general numerical approach we have created, for example, aperiodic arrays that exhibit local n-fold rotational symmetry, with $n = 40$ and 120 (Supplementary Information). We have also created other, more exotic, aperture array structures that do not exhibit any n-fold rotational symmetry, but nevertheless exhibit resonant transmission bands (T.M., A.A., A.N. and Z.V.V., unpublished results).

Our results show that the THz transmission spectra obtained using quasiperiodic, as well as more generalized aperiodic, aperture structures in metal films also possess enhanced transmission resonances with lineshapes that are comparable in width to those of resonances obtained with periodic structures[7]. We also show that these resonances can be engineered to yield desirable transmission properties. Further exploration of these structures is expected to lead to new optoelectronic device embodiments[21] that are expected to be particularly important in the THz spectral range, which is largely devoid of usable optoelectronic devices.

Received 14 June 2006; accepted 19 January 2007.

1. Ebbesen, T. W., Lezec, H. J., Ghaemi, H. F., Thio, T. & Wolff, P. A. Extraordinary optical transmission through sub-wavelength hole arrays. *Nature* **391,** 667–669 (1998).
2. Barnes, W. L., Dereux, A. & Ebbesen, T. W. Surface plasmon subwavelength optics. *Nature* **424,** 824–830 (2003).
3. Ghaemi, H. F., Thio, T., Grupp, D. E., Ebbesen, T. W. & Lezec, H. J. Surface plasmons enhance optical transmission through subwavelength holes. *Phys. Rev. B* **58,** 6779–6782 (1998).
4. Genet, C., van Exter, M. P. & Woerdman, J. P. Fano-type interpretation of red shifts and red tails in hole array transmission spectra. *Opt. Commun.* **225,** 331–336 (2003).
5. Garcia de Abajo, F. J., Saenz, J. J., Campillo, I. & Dolado, J. S. Site and lattice resonances in metallic hole arrays. *Opt. Express* **14,** 7–18 (2006).
6. Janot, C. *Quasicrystals: A Primer* 2nd edn (Oxford Univ. Press, New York, 1994).
7. Cao, H. & Nahata, A. Influence of aperture shape on transmission properties of a periodic array of subwavelength apertures. *Opt. Express* **12,** 3664–3672 (2004).

8. Kaliteevski, M. A. *et al.* Diffraction and transmission of light in low-refractive index Penrose-tiled photonic quasicrystals. *J. Phys. Condens. Matter* **13,** 10459–10470 (2001).
9. Oxborrow, M. & Henley, L. C. Random square-triangle tilings: A model for twelve fold-symmetric quasicrystals. *Phys. Rev. B* **48,** 6966–6998 (1993).
10. Bethe, H. A. Theory of diffraction by small holes. *Phys. Rev.* **66,** 163–182 (1944).
11. Agrawal, A. & Nahata, A. Time-domain radiative properties of a single subwavelength aperture surrounded by an exit side surface corrugation. *Opt. Express* **14,** 1973–1981 (2006).
12. Penrose, R. The role of aesthetics in pure and applied mathematical research. *Bull. Inst. Math. Appl.* **10,** 266–271 (1974).
13. Zoorob, M. E., Charlton, M. D. B., Parker, G. J., Baumberg, J. J. & Netti, M. C. Complete photonic bandgaps in 12-fold symmetric quasicrystals. *Nature* **404,** 740–743 (2000).
14. Sun, M. *et al.* The role of periodicity in enhanced transmission through subwavelength hole arrays. *Chin. Phys. Lett.* **23,** 486–488 (2006).
15. Przybilla, F., Genet, C. & Ebbesen, T. W. Enhanced transmission through Penrose subwavelength hole arrays. *Appl. Phys. Lett.* **89,** 121115 (2006).
16. Koerkamp, K. J. K., Enoch, S., Segerink, F. B., van Hulst, N. F. & Kuipers, L. Strong influence of hole shape on extraordinary transmission through periodic arrays of subwavelength holes. *Phys. Rev. Lett.* **92,** 183901 (2004).
17. Fano, U. Effects of configuration interaction on intensities and phase shifts. *Phys. Rev.* **124,** 1866–1873 (1961).
18. Österbacka, R., Jiang, X. M., An, C. P., Horovitz, B. & Vardeny, Z. V. Photoinduced quantum interference antiresonances in π-conjugated polymers. *Phys. Rev. Lett.* **88,** 226401 (2002).
19. Sarrazin, M., Vigneron, J. P. & Vigoureux, J. M. Role of Wood anomalies in optical properties of thin metallic films with bidimensional array of subwavelength holes. *Phys. Rev. B* **67,** 085415 (2003).
20. Lee, T. D. M., Parker, G. J., Zoorob, M. E., Cox, S. J. & Charlton, M. D. B. Design and simulation of highly symmetric photonic quasi-crystals. *Nanotechnology* **16,** 2703–2706 (2005).
21. Matsui, T., Agrawal, A., Nahata, A. & Vardeny, Z. V. Enhanced transmission properties of aperiodic aperture arrays in metallic and semiconductor films and their application to optoelectronic devices. *University of Utah Patent Disclosure*, (2006).

Supplementary Information is linked to the online version of the paper at www.nature.com/nature.

Acknowledgements This work was supported in part by the Army Research Office and the SYNERGY programme at the University of Utah.

Author Information Reprints and permissions information is available at www.nature.com/reprints. The authors declare no competing financial interests. Correspondence and requests for materials should be addressed to Z.V.V. (val@physics.utah.edu) or A.N. (nahata@ece.utah.edu).